



THE EXPERIMENTAL MODELING OF GFRP CONFINED CONCRETE CYLINDERS SUBJECTED TO AXIAL LOADS

MEHDI BAKHSHI¹, BAHAREH ABDOLLAHI², MASOUD MOTAVALLI³,
MOHAMMAD SHEKARCHIZADE⁴ AND MEHDI GHALIBAFIAN⁵

ABSTRACT

Seismic repair, rehabilitation and strengthening of existing structures have become a major part of construction activities. It is now well known that both strength and ductility of concrete compressive members can be greatly improved by using glass fiber reinforced polymer (GFRP) sheets. The objectives of this study are to investigate the effects of three parameters on the stress-strain behavior of GFRP confined concrete. The parameters studied in this research included unconfined concrete core strength, number of layers of GFRP and the fiber orientation in the laminate structure. The confinement and ductility effectiveness along with energy absorption capacity are studied based on the experimental results. Due to recent increase in the application of high performance concrete structures, compressive behavior of high strength concrete columns externally confined by FRP jackets are focused. Although many confinement models have been developed in order to predict the response of confined concrete, their applications are limited providing different degrees of prediction accuracy. In this paper, three confinement models with the applicability of predicting complete stress-strain response of FRP confined concrete are evaluated and discussed according to the experimental results.

1 INTRODUCTION

Fiber reinforced polymer (FRP) jackets provide an effective retrofit strategy for structurally deficient concrete columns. The majority of structural deficiencies in existing concrete columns can be attributed to lack of transverse reinforcement. This is especially true for columns in seismically active regions, designed prior to the enactment of modern seismic codes. Columns with insufficient transverse reinforcement suffer; i) brittle crushing of unconfined concrete, ii) premature shear failure and iii) reinforcement splice failure if the longitudinal reinforcement is spliced at or near a potential plastic hinge region. FRP sheets provide an excellent opportunity to enhance column resistance in all three areas of weakness. In this paper, effectiveness of Glass Fiber Reinforced Polymer (GFRP) jackets in preventing

¹ PhD Student, Civil and Environmental Eng. Dept., Arizona State University, Tempe, AZ
Zip Code: 85281, e-mail: mbakhshi@asu.edu

² Graduate Research Assistant, University of Tehran, Iran

³ Structural Lab chair, EMPA, Federal Laboratories for Materials Testing and Research, Switzerland

⁴ Assistant Professor, University of Tehran, Iran

⁵ Late Associate Professor, University of Tehran, Iran

brittle crushing of unconfined concrete is studied. An experimental program was developed to investigate effects of three parameters on the stress-strain behavior of GFRP confined concrete. The parameters studied in this research include unconfined concrete core strength, number of layers of GFRP and the fiber orientation in the laminate structure. The confinement and ductility effectiveness along with energy absorption capacity are studied based on the experimental results. Finally, three confinement models with the applicability of predicting complete stress-strain response of FRP confined concrete are evaluated and discussed according to the experimental results.

2 EXPERIMENTAL PROGRAM

The experimental program consisted of axial compressive tests on plain concrete and GFRP confined concrete cylinders. A total of 14 GFRP confined and 6 unconfined control concrete cylinders with a diameter of 150 mm and a height of 300 mm were tested. The experimental program included three parameters: unconfined concrete core strength, number of layers of GFRP and the fiber orientation. For each parameter being considered, two identical samples were prepared for repeatability verification.

Table 1 presents the specifications of different GFRP confined specimens.

The effect of unconfined concrete core strength was examined by using three target strengths of 10, 20 and 40 MPa. However, the average strengths of concrete batches were 14.8, 25.1 and 41.7 MPa, respectively. The low, normal and high strength concrete cylinders were wrapped with one layer of GFRP sheet with 0° fiber orientation with respect to the hoop direction. The effect of number of layers of GFRP sheet was studied by using three different numbers of layers. The 20 MPa concrete cylinders were confined with 1, 2 and 4 layers of GFRP sheet with 0° fiber orientation with respect to the hoop direction. The effect of fiber orientation was examined by wrapping the 20 MPa concrete cylinders with 2 layers of GFRP sheet and three different ply configurations. For the first configuration, the 2 layers were placed with 0° fiber orientation with respect to the hoop direction. For the second configuration, the first layer was placed with 0° and the second layer with 90° fiber orientation with respect to the hoop direction. For the third configuration, the first layer was placed with -45° and the second layer with 45° fiber orientation with respect to the hoop direction. The three ply configurations discussed above, are briefly presented as $0^\circ/0^\circ$, $0^\circ/90^\circ$ and $-45^\circ/+45^\circ$ fiber orientation, respectively.

TABLE 1. Details of GFRP confined specimens

Specimen	Core Strength	Number of layers	Ply configuration
	(Mpa)		
F1-A	10	1	0°
F1-B			
F2-A	20	1	0°
F2-B			
F3-A	40	1	0°
F3-B			
F4-A	20	2	$0^\circ / 0^\circ$
F4-B			
F5-A	20	4	$0^\circ / 0^\circ / 0^\circ / 0^\circ$
F5-B			
F6-A	20	2	$0^\circ / 90^\circ$
F6-B			
F7-A	20	2	$-45^\circ / +45^\circ$
F7-B			

2.1 Materials

Three different concrete strengths were obtained by using different cement content and water to cement ratios. The proportion of the mixtures is presented in Table 2. The glass fiber fabric used for confinement of cylinders was SikaWrap Hex 430G. A unidirectional Glass Fiber Reinforced Polymer (GFRP) was produced by hand layup technique using this product with Sikadur 300 epoxy. Table 3 shows the mechanical properties of the cured laminate GFRP sheet, based on coupon tests using ASTM D 3039 standard. The design values are calculated using the average values of test series minus two standard deviations. The given data are available in the technical data sheet of the product, at the related site of SIKA.

TABLE 2. Concrete mixture proportions

Specimen ID	Concrete Core Type	Cement	Water	w/c	Super Plasticizer	Corse Aggregate	Fine Aggregate
		(kg/m ³)	(kg/m ³)		(%)	(kg/m ³)	(kg/m ³)
C10	Low strength	200	120	0.6	-	832	1248
C20	Normal strength	250	125	0.5	-	815	1213
C40	High strength	400	140	0.3	2	741	1111

TABLE 3. The cured laminate properties of GFRP sheet

Property	Tensile Strength	Tensile Modulus	Tensile Elongation	90° Tensile Strength	90° Tensile Modulus	90° Tensile Elongation	Ply Thickness
	(MPa)	(MPa)	(%)	(MPa)	(MPa)	(%)	(mm)
Average Value	537	26493	2.21	23	7069	0.46	0.508
Design Value	504	24591	1.93	15	5978	0.40	-

2.2 Fabrication of specimens

Standard Cylinders with 300 mm height and 150 mm diameter were used to determine the compressive behavior of unconfined concrete cores and also to prepare concrete cores with different strengths to be confined. After the specimens were cast, compacted and finished, they were covered with a wet burlap cloth, and were left in forms for 1 day. After demolding, all specimens were cured in the water for 28 days. The control specimens were capped and tested after being air-dried at the age of 28 days. The specimens to be confined were left in the laboratory for 7 days to be prepared for strengthening at the age of 35 days.

The surface of the concrete cylinders should be clean and sound before being wrapped. The surface may be dry or damp but free of standing water. Therefore, existing dust, oil or curing was removed from the surface of the concrete cylinders. Then GFRP sheet was prepared with an extra length of about a quarter of specimen perimeter to provide an overlap. This led to a length of 600 mm in the hoop direction for each layer of GFRP. This was used to insure adequate bond and continuity of the jacket in the fiber direction. After pre-mixing each component of epoxy resin, the contents of part B were poured into part A with a certain proportion. Then the epoxy resin was prepared by thoroughly mixing two components for 5 minutes, until they were uniformly blended.

The wet lay-up technique was used to wrap the concrete specimens with GFRP sheets. This technique started with applying a layer of resin to the dry surface of the concrete cylinder. Then the GFRP sheet was

fully impregnated with the resin by using a brush. The viscosity of the resin was proper to wet through the fabric without excessive running. Then the presaturated sheet was applied to the resin-wetted concrete surface such that the fibers were oriented in the desired direction. The surface was pressed with a roller or brush in the fiber direction to remove the entrapped air and ensure proper bond with the concrete. Next, another layer of resin was applied on the first layer and additional layers were applied, if required. After the specimens were confined, they were left in laboratory conditions for 14 days after gluing to be completely cured. At the age of 49 days, the specimens were capped using an appropriate plaster prior to testing. The result was that the loading faces of the cylinders were parallel and sufficiently smooth to eliminate the probable stress concentration (ACI Committee 440 2002).

2.3 Test setup and testing procedure

All specimens were tested by MTS universal machine and a data acquisition system. Loading was applied monotonically in a displacement control mode with a constant rate of 1 mm/min, which corresponds to a strain rate of 0.0033 per min. The load was applied to the entire cross section, including the concrete core and the GFRP jacket. The assembled computer data acquisition system was used to record the data. The values of displacements between the loading platens were used for obtaining complete stress-strain curves. The specimens were loaded almost up to the strain at which all of the specimens were softened. Figure 1 shows the test set up with a concrete cylinder under compressive loading.



FIGURE 1. Test set up

3 EXPERIMENTAL RESULTS

Compressive stress-strain responses are shown in Figure 2. Each graph represents the behavior of two identical specimens tested and the average behavior obtained for each case. For low to medium concrete strengths, the stress-strain curves showed a typical bilinear trend with strain hardening. This is attributed to the fact that once the concrete reaches its unconfined strength, it starts to dilate excessively due to the development of a uniform network of internal microcracks, and the jacket becomes fully activated in confinement. The strains increase rapidly as evident from the second slope of the stress-strain curve. For medium to high concrete strengths, as the unconfined concrete strength increases, the second part of the bilinear curve gradually shifts from strain hardening to a flat plateau, and eventually to a sudden strain softening with a drastically reduced ductility. For high strength concrete, confining the cylinders with

GFRP sheets does not significantly change the stress-strain behavior of confined concrete from that of unconfined concrete except for a limited increase in compressive strength and ductility.

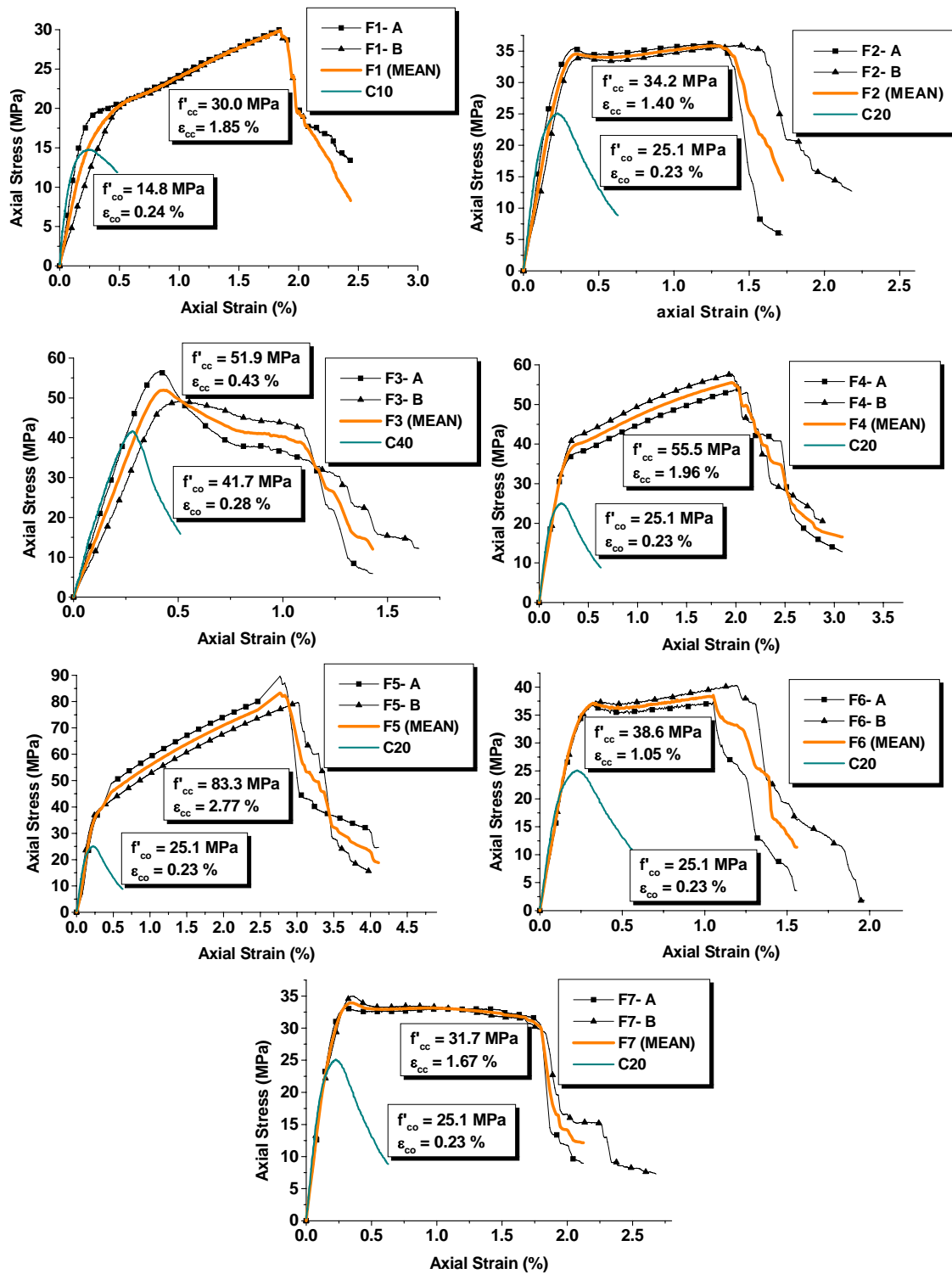


FIGURE 2. Compressive stress-strain behavior of GFRP confined and unconfined specimens

3.1 Effect of unconfined concrete strength

Concretes with compressive strengths of 10, 20 and 40 MPa were representatives of low, normal and high strength concretes. For determining the effect of concrete core strength, 1 layer of GFRP with 0° fiber orientation with respect to the hoop direction was used to confine the cylinders. The effects of different concrete strengths on compressive stress-strain behavior were shown in Figure 3 and Table 4. The values of the major parameters are measured for all the specimens. The ratios of these parameters to those measured for unconfined concrete cylinders show the improvements in compressive properties of confined concrete due to the effects of confinement. The energy absorption was measured for all specimens by integrating the area under each stress-strain curve up to the strain corresponding to the maximum strength. The energy absorption capacity of GFRP wrapped specimens also indicates the effectiveness of GFRP confinement.

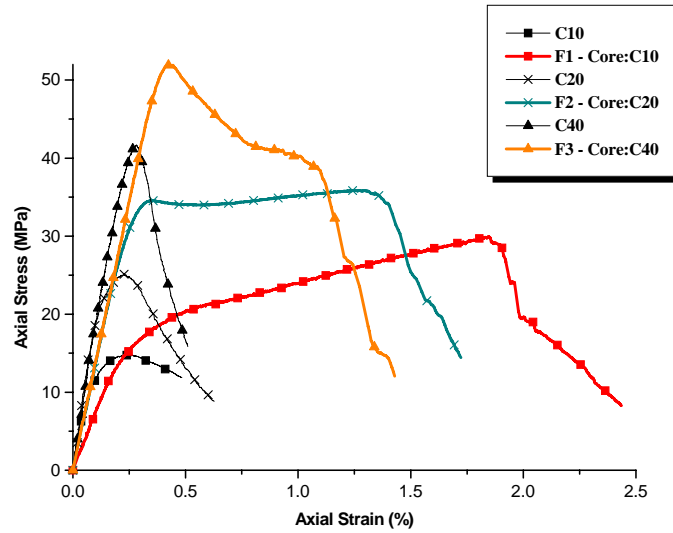


FIGURE 3. Effect of unconfined concrete strength in the behavior of confined concrete cylinders

TABLE 4. Effect of unconfined concrete strength on compressive properties of confined cylinders

Specimen	Core Strength	Number of layers	Fiber Orientation	f_{co}	f_{cc}	f_{cc}/f_{co}	Difference to the 1st Case (%)	Difference to the 2nd Case (%)
	(Mpa)			(Mpa)	(Mpa)			
F1	10	1	0°	14.8	30.0	2.03		
F2	20	1	0°	25.1	34.2	1.36	-33	
F3	40	1	0°	41.7	51.9	1.25	-39	-8

Specimen	Core Strength	Number of layers	Fiber Orientation	ϵ_{co}	ϵ_{cc}	$\epsilon_{cc}/\epsilon_{co}$	Difference to the 1st Case (%)	Difference to the 2nd Case (%)
	(Mpa)			(%)	(%)			
F1	10	1	0°	0.24	1.85	7.71		
F2	20	1	0°	0.23	1.40	6.09	-21	
F3	40	1	0°	0.28	0.43	1.54	-80	-75

Specimen	Core Strength	Number of layers	Fiber Orientation	Confined Absorbed Energy (MJ/m ³)	Unconfined Absorbed Energy (MJ/m ³)	Absorbed Energy Enhancement
	(Mpa)					
F1	10	1	0°	0.407	0.027	15
F2	20	1	0°	0.439	0.039	11
F3	40	1	0°	0.124	0.068	2

The experiments indicated that the increase in the compressive strength of GFRP confined specimens compared to the unconfined specimens was 103%, 36% and 25% for concrete cores with the strength of 10, 20 and 40 MPa, respectively. The maximum strain or ductility of GFRP confined specimens compared to the unconfined specimens showed 671%, 509% and 54% increase for low, normal and high strength concrete cores, respectively. The same trend was also observed for the absorbed energy where 1407%, 1026% and 82% increase was found for low, normal and high strength concrete cores, respectively.

Figure 4 shows a plot of the confinement effectiveness (f'_{cc}/f'_{co}) and ductility effectiveness ($\epsilon_{cc}/\epsilon_{co}$) versus the unconfined concrete strength f'_{co} for the specimens confined with one layer of GFRP wrap with 0° fiber orientation with respect to the hoop direction. Each value represents the average value of the two identical cylinders tested under compression. It is evident that as the unconfined concrete strength increases, the confinement effectiveness decreases. The GFRP wrapped cylinders with the least concrete core strength show the maximum increase in confined strength. The figure also reflects the reduction of ductility effectiveness of GFRP wraps in high strength concrete.

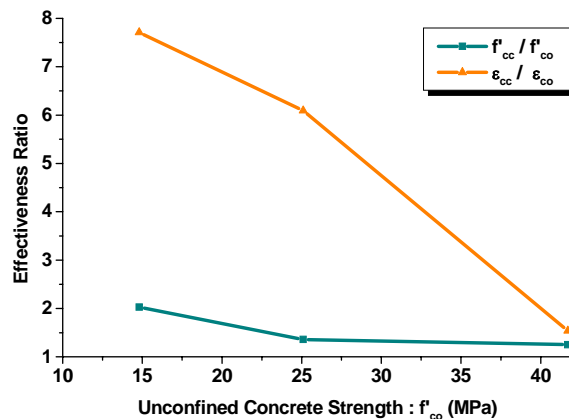


FIGURE 4. Effect of unconfined strength of concrete on confinement and ductility effectiveness ratio

3.2 Effect of number of layers

The effects of different number of layers of GFRP on compressive stress-strain behavior were shown in Figure 5 and Table 5. The effect of number of layers of GFRP in a confining jacket was examined using three sets of number of layers including 1, 2 and 4 layers of GFRP resulting in the jacket thickness equal to 0.508, 1.016 and 2.032 mm, respectively. These levels were chosen to examine the sensitivity of GFRP jacket thickness on compressive behavior of confined specimens. In this comparison, the concrete core strength was 20 MPa and the fiber orientation was chosen 0° with respect to the hoop direction.

As expected, the experiments indicated that any increase in GFRP jacket thickness caused an increase in both maximum stress and strain and also in the absorbed energy of the strengthened specimens. The maximum stress and strain obtained among all specimens tested in this study was related to the specimens confined with the 4-layer GFRP jacket with the values of 83.3 MPa and 2.77%, respectively. The increase in the jacket thickness from 1 layer to 2 layers and 4 layers translated 36%, 121% and 231% strength increase compared to the unconfined specimens. The same trend existed when the ductility increased by 509%, 752% and 1104% and absorbed energy increased by 11, 22 and 42 times.

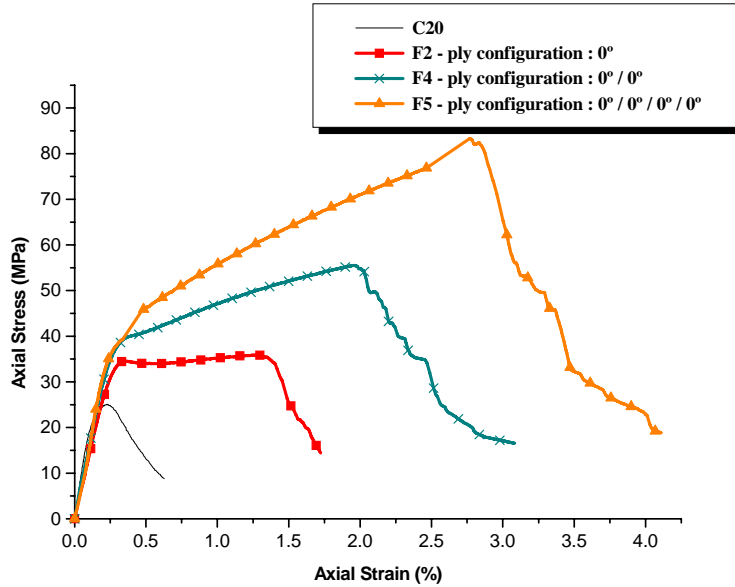


FIGURE 5. Effect of number of GFRP layers in the behavior of confined concrete cylinders

TABLE 5. Effect of number of GFRP layers on compressive properties of confined concrete cylinders

Specimen	Core Strength	Number of layers	Fiber Orientation	f_{co}	f_{cc}	f_{cc}/f_{co}	Difference to the 1st Case (%)	Difference to the 2nd Case (%)
	(Mpa)			(Mpa)	(Mpa)			
F2	20	1	0°	25.1	34.2	1.36		
F4	20	2	0° / 0°	25.1	55.5	2.21	62	
F5	20	4	0° / 0° / 0° / 0°	25.1	83.3	3.31	144	50

Specimen	Core Strength	Number of layers	Fiber Orientation	ϵ_{co}	ϵ_{cc}	$\epsilon_{cc}/\epsilon_{co}$	Difference to the 1st Case (%)	Difference to the 2nd Case (%)
	(Mpa)			(%)	(%)			
F2	20	1	0°	0.23	1.40	6.09		
F4	20	2	0° / 0°	0.23	1.96	8.52	40	
F5	20	4	0° / 0° / 0° / 0°	0.23	2.77	12.04	98	41

Specimen	Core Strength	Number of layers	Fiber Orientation	Confined Absorbed Energy (MJ/m ³)	Unconfined Absorbed Energy (MJ/m ³)	Absorbed Energy Enhancement
	(Mpa)					
F2	20	1	0°	0.439	0.039	11
F4	20	2	0° / 0°	0.862	0.039	22
F5	20	4	0° / 0° / 0° / 0°	1.634	0.039	42

3.3 Effect of fiber orientation

The effect of fiber orientation of GFRP in a confining jacket was examined using three sets of fiber orientations. In this comparison, the concrete core strength was 20 MPa and the cylinders were confined with 2 layers of GFRP sheet. The fiber orientations included 0°/0°, 0°/90° and -45°/+45°. These configurations were chosen to study the effects of 0°, 45° and 90° fiber orientations with respect to the

loading direction on the confined behavior of specimens. The effects of fiber orientation of layers on compressive stress-strain behavior of confined concrete were shown in Figure 6 and Table 6.

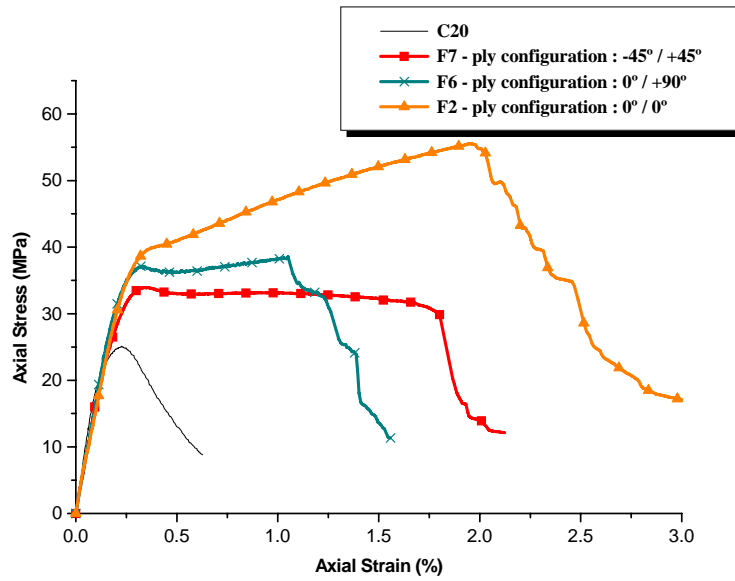


FIGURE 6. Effect of fiber orientation in the behavior of confined concrete cylinders

TABLE 6. Effect of fiber orientation on compressive properties of confined concrete cylinders

Specimen	Core Strength	Number of layers	Fiber Orientation	f_{co}	f_{cc}	f_{cc}/f_{co}	Difference to the 1st Case (%)	Difference to the 2nd Case (%)
	(Mpa)			(Mpa)	(Mpa)			
F4	20	2	0° / 0°	25.1	55.5	2.21		
F6	20	2	0° / 90°	25.1	38.6	1.54	-30	
F7	20	2	-45° / +45°	25.1	31.7	1.26	-43	-18

Specimen	Core Strength	Number of layers	Fiber Orientation	ϵ_{co}	ϵ_{cc}	$\epsilon_{cc}/\epsilon_{co}$	Difference to the 1st Case (%)	Difference to the 2nd Case (%)
	(Mpa)			(%)	(%)			
F4	20	2	0° / 0°	0.23	1.96	8.52		
F6	20	2	0° / 90°	0.23	1.05	4.57	-46	
F7	20	2	-45° / +45°	0.23	1.67	7.26	-15	59

Specimen	Core Strength	Number of layers	Fiber Orientation	Confined Absorbed Energy (MJ/m ³)	Unconfined Absorbed Energy (MJ/m ³)	Absorbed Energy Enhancement
	(Mpa)					
F4	20	2	0° / 0°	0.862	0.039	22
F6	20	2	0° / 90°	0.346	0.039	9
F7	20	2	-45° / +45°	0.513	0.039	13

The sample with 0°/0° jacket is sufficiently confined and the second part of the stress-strain curve is ascending, while this ascending part shifts to a plateau in two other cases. This different behavior resulted in 121%, 752% and 2200% increase compared to the unconfined specimens in maximum stress, maximum strain and energy absorption capacity, for the specimens confined with 0°/0° GFRP jacket, respectively. This increase was 54%, 357% and 900% for the 0°/90° ply configuration and 26%, 626% and 1300% for the -45°/+45° ply configuration, respectively. The 0°/90° jacket provided a higher confined strength than the jacket with -45°/+45° ply configuration. However, the ultimate confined strain and the

absorbed energy for the specimens with $-45^{\circ}/+45^{\circ}$ jacket were higher than the specimens with $0^{\circ}/90^{\circ}$ jacket.

4 COMPARISON WITH CONFINEMNET MODELS

Figure 7 shows an assessment of confinement models in comparison with the experimental results. Three models are chosen for comparison with the experimental results. These models which predict the complete stress-strain behavior of confined concrete specimens are summarized below.

4.1 Summery of models

The Model by Toutanji (Toutanji 1999) predicts the entire stress-strain behavior of confined concrete. The empirical expressions are formed to define two distinct regions with an intersection point at the lateral strain of 0.002. The Model by Spoelstra and Monti (Spoelstra and Monti 1999) is based on a rotational iterative procedure to determine the full stress-strain behavior of confined concrete. The empirical equations are used for determining the lateral confinement pressure at any strain level. The model accounts for the continuous interaction between the confining jacket and the dilating concrete core. The Model by Fam and Rizkalla (Fam and Rizkalla 2001) is based on the equilibrium conditions and compatibility of radial displacements to form an expression for lateral confinement pressure. The confinement pressure is a function of the Poisson's ratio and modulus of the concrete and the confining jacket. The model accounts for the biaxial state of stress in the confining jacket by using Tsai-Wu failure criterion.

4.2 Application of models

It can be seen from Figure 7 that the existing models predict the stress-strain behavior of confined concrete with different degrees of accuracy for the low to high strength concrete and different jacket thicknesses. For concrete with low strength (specimen F1), the models provide a relatively good prediction of the stress-strain behavior. For concrete with medium strength, the stress-strain behavior is relatively well predicted for specimens confined with 2 and 4 layers of GFRP. However, for the specimen with 1 layer of GFRP (specimen F2) in which the jacket is not stiff enough, the experimental curve shows a plateau for the second part of the behavior, while the models show an ascending response. For high strength concrete (specimen F3), the existing models predict the initial ascending part of the stress-strain behavior, but they failed to predict the behavior when the confined concrete reaches the pick strength. Beyond this point, the models show a strain hardening response while the experimental curve shows a descending stress-strain behavior.

It can be noted that all models provided a relatively good prediction of the peak confined strength, but they all overestimated the ultimate confined strain for different types of concrete strengths and GFRP jacket thicknesses. However, the model by Toutanji shows the best prediction of the ultimate confined strain. The model by Fam and Rizkalla shows a similar behavior to the experimental results except for high strength concrete. This similarity is the result of accounting the biaxial state of stress in GFRP jacket, but there exists a uniform decrease in strength at any certain strain level compared to the experiments.

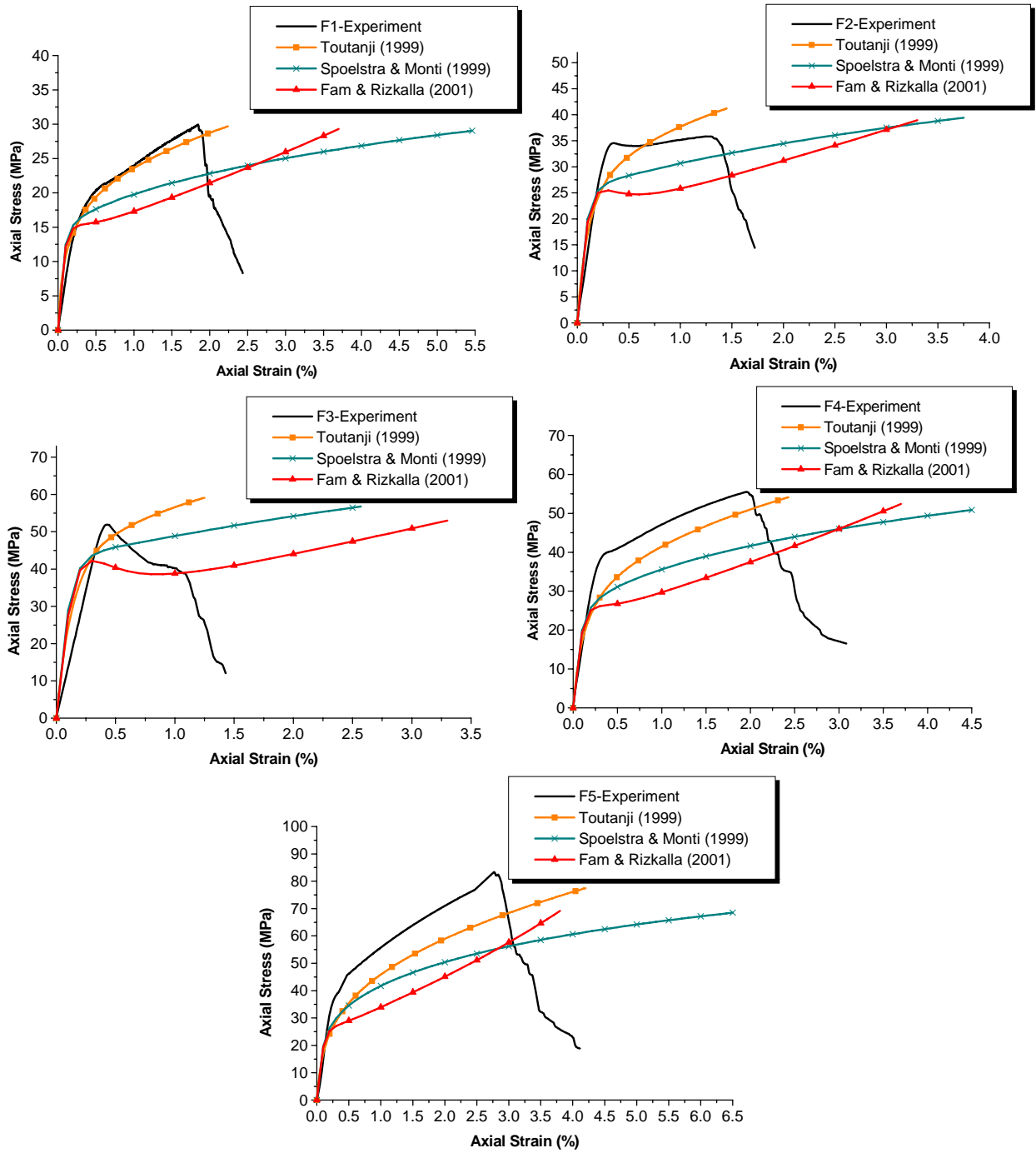


FIGURE 7. Comparison of confinement models with the experimental results

5 CONCLUSIONS

The following conclusions are deduced from the experimental results and the evaluation of three confinement models:

- Confined specimens with low to medium strength concrete show bilinear stress-strain responses. Confining low to medium strength concrete cylinders leads to significant enhancement in strength and ductility.
- The confined high strength concrete shows a strain softening response and very little ductility when it reaches the unconfined concrete strength level and no distinct post peak behavior is observed. For the case of confined high strength concrete, the response is quite similar to that of unconfined concrete. For high strength concrete, little improvement in strength can be achieved due to the confinement, but no significant improvement in ductility is expected.
- For new construction with FRP tubes, it is more effective and economical to use low or medium strength concrete instead of high strength concrete.
- The confinement effectiveness, the ductility effectiveness and the energy absorption capacity reduce with increase in the unconfined concrete strength.
- The ratio of confinement effectiveness and ductility effectiveness reach to a relatively same level in case of confining high strength concrete.
- The confinement effectiveness, the ductility effectiveness and the energy absorption capacity proportionally improve with the increase in the number of GFRP layers.
- The sample with $0^{\circ}/0^{\circ}$ jacket is sufficiently confined and the second part of the stress-strain curve is ascending. The second part of the stress-strain response shifts to a plateau in the case of confined specimens with $0^{\circ}/90^{\circ}$ and $-45^{\circ}/+45^{\circ}$ ply configuration.
- The $0^{\circ}/90^{\circ}$ jacket provided a higher confined strength than the jacket with $-45^{\circ}/+45^{\circ}$ ply configuration.
- The ultimate confined strain and the absorbed energy for the specimens with $-45^{\circ}/+45^{\circ}$ jacket were higher than the specimens with $0^{\circ}/90^{\circ}$ jacket.
- The confinement models show different degrees of accuracy in predicting the confined concrete behavior. For medium concrete strength, the confinement models provided a better prediction of stress-strain response in case of the higher number of layers of GFRP.
- The confinement models failed to predict the stress-strain response of confined high strength concrete.
- The confinement models provided a relatively good prediction of the peak confined strength, but they overestimated the ultimate confined strain for different types of concrete strengths and GFRP jacket thicknesses.

ACKNOWLEDGEMENTS

The authors wish to acknowledge financial support provided by Radyab Co., Tehran, Iran.

REFERENCES

- [1] ACI Committee 440, 2002. "Guide for the Design and Construction of Externally Bonded FRP systems for Strengthening of Concrete Structure", *ACI 440.2R-02*, American Concrete Institute, Farmington Hill, Mich., 2002, pp. 27-28.
- [2] Fam, A. Z. and Rizkalla, S. H., 2001. "Confinement Model for Axially Loaded Concrete Confined by Circular Fiber-Reinforced Polymer Tubes", *ACI Structural Journal*, 98, 4, 2001, pp 451-461.
- [3] Spoelstra, M. R. and Monti, G., 1999. "FRP-Confined Concrete Model", *Journal of Composites for Construction*, ASCE, 3, 3, 1999, pp 143-150.
- [4] Toutanji, H. A., 1999. "Stress-Strain Characteristics of Concrete Columns Externally Confined with Advanced Fiber Composite Sheets", *ACI Materials Journal*, 96, 3, 1999, pp 397-404.